

Acta Crystallographica Section B

**Structural
Science**

ISSN 0108-7681

Two fluoradene derivatives: pseudosymmetry, eccentric ellipsoids and a phase transition

Aibing Xia, John P. Selegue, Alberto Carrillo, Brian O. Patrick, Sean Parkin and Carolyn Pratt Brock

CORRECTED REPRINT

Copyright © International Union of Crystallography

This is a corrected reprint of a paper by Xia et al. [*Acta Cryst.* (2001). B57, 507–516].

Two fluoradene derivatives: pseudosymmetry, eccentric ellipsoids and a phase transition

Aibing Xia, John P. Selegue,
Alberto Carrillo, Brian O.
Patrick, Sean Parkin and
Carolyn Pratt Brock*

Department of Chemistry, University of
Kentucky, Lexington, KY 40506-0055, USA

Correspondence e-mail: cpbrock@pop.uky.edu

Received 27 November 2000

Accepted 25 May 2001

Structures of two derivatives of the curved fluoradene ring system ($C_{19}H_{12}$) have been determined. Both have phases that are highly pseudosymmetric. At room temperature crystals of *7b*-triisopropylsilylfluoradene ($C_{28}H_{32}Si$) have a $P\bar{1}$ cell that contains two independent molecules ($Z' = 2$) and that is almost centered. Crystals of *7b*-(2,4-dinitrophenyl)fluoradene ($C_{25}H_{14}N_2O_4$) have both a $P2_1/c$ cell with $Z' = 1$ and a $P2_1/c$ cell with $Z' = 2$. The molecular volumes in these two $P2_1/c$ structures differ by 0.7%, but the structures are otherwise virtually the same; the two independent molecules in the larger cell are related by a pseudotranslation. Some of the atomic ellipsoids in the $P2_1/c$, $Z' = 1$ structure are very large and eccentric, and there are some hints in the diffraction pattern of an incipient phase transition, but the $Z' = 1$ and $Z' = 2$ phases are clearly different. The $P2_1/c$, $Z' = 2$ crystal at 295 K probably contains some volume fraction of the $Z' = 1$ phase; when the temperature is lowered to 273 K this fraction is decreased markedly. The pronounced pseudosymmetry in the $P\bar{1}$ and $P2_1/c$ structures that have $Z' = 2$ has been investigated by analysing the atomic coordinates, by performing refinements in the smaller pseudocells and by making separate Wilson plots for the classes of reflections which are systematically strong and systematically weak. All three approaches are informative, but they reveal different information. Least-squares fits of coordinates of corresponding atoms measure the similarity of the molecular conformations. The Wilson plots allow a quantitative comparison of the intensities of the strong and weak reflections and thus an assessment of the deviations of the true structure from the smaller pseudocell structure. Comparison of the atomic displacements obtained in the full and pseudocell refinements shows where the structural distortions are largest and provides an indication of their directions."

1. Introduction

Pseudosymmetric structures with $Z' > 1$ (more than one molecule in the asymmetric unit) are frequently viewed with suspicion. Structures with large and/or eccentric atomic displacement ellipsoids are also viewed skeptically. These problems are illustrated by two structures we have determined recently (see Fig. 1) in connection with another project (Xia, 1998; Xia *et al.*, 2000). The structures also raise questions about polymorphism and symmetry-lowering phase transitions.

The structure at room temperature of *7b*-triisopropylsilylfluoradene (hereafter, FLTIPS) is sufficiently pseudosym-

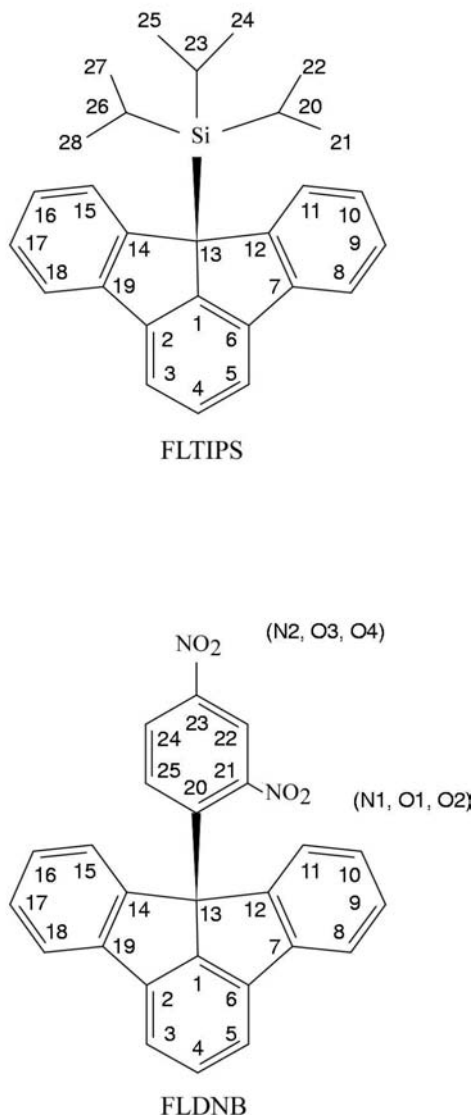


Figure 1
Chemical line drawings that show the atom-numbering schemes. Corresponding atoms in different molecules are distinguished by a final letter (A or B).

metric that it has triggered warning messages in crystallographic checking programs. The choice of the larger unit cell is, however, unambiguous because the half of the reflections that would be absent if the pseudotranslation were exact are clearly present although weak. Least-squares refinement in a pseudocell using only half of the data leads to a structure that many journals would consider acceptable, but refinement in the larger cell is clearly better. Comparison of the averaged and actual structures reveals the very small distortions associated with the cell doubling.

At room temperature the structure of 7*b*-(2,4-dinitrophenyl)fluoradene (hereafter, FLDNB) was found initially to be in space group $P2_1/c$ with $Z' = 1$, but the C-atom ellipsoids of the fluoradene moiety are *much* larger and more

eccentric than those of the Si atom or of the C, N and O atoms of the dinitrophenyl ring. Careful inspection of the scattering suggested an incipient phase transition involving a doubling of the *a* axis. Data were later collected at 295, 273 and 250 K for a crystal (hereafter, FLDNB2), which has a very similar unit cell except for a doubling of the *a* axis and of Z' . At 250 K the ellipsoids of all the atoms of the FLDNB2 phase are unexceptional, but the structure is still strongly pseudosymmetric.

2. Experimental

Results are presented (Table 1; Figs. 2–4) for five structure determinations: FLTIPS at 294 K, FLDNB at 293 K and FLDNB2 (the second polymorph) at (a) 295, (b) 273 and (c) 250 K. Results are also presented (Table 1; Figs. 2 and 3; see below) for pseudocell refinements of the structures FLTIPS and FLDNB2A (295). All reflection intensities were measured using a Nonius KappaCCD diffractometer and graphite-monochromated Mo $K\alpha$ radiation ($\lambda = 0.71073 \text{ \AA}$) under control of the program *COLLECT* (Nonius, 1998). Cells were determined and the data reduced with *DENZO-SMN* (Otwinowski & Minor, 1997). The structures were solved with the program *SIR92* (Altomare *et al.*, 1994) or with *SHELXS97* (Sheldrick, 1997*a*) and were refined on F^2 with *SHELXL97* (Sheldrick, 1997*b*). The H atoms were placed in idealized positions recalculated after every cycle. Programs used to prepare material for publication included *SHELXTL/PC* (Sheldrick, 1990) and CIF-processing macros written locally.

Details specific to the individual compounds are given below. All other structural information has been deposited.¹

2.1. FLTIPS

Crystals were grown at 263 K from a pentane solution. Data were measured first at room temperature on a Nonius CAD4 diffractometer. The crystal was found to be triclinic with $Z' = 2$, but the data were so weak [only 36% of all reflections had $I > 2\sigma(I)$] that the structure determination was abandoned after the connectivity had been established (Xia, 1998). About a year later, after installation of a Nonius KappaCCD diffractometer, another crystal was examined at 294 (1) K. The unit cell was the same as found previously, but the fraction of data having $I > 2\sigma(I)$ rose to 89%. Some of the increase can be attributed to the greater X-ray power (50 kV, 30 mA *versus* 40 kV, 20 mA) and some of the increase may possibly be attributed to crystal size (the dimensions of the first crystal have been lost), but the remaining increase is instrument dependent. Data collection time was also reduced sharply (from 125 to 18 h).

The structure is approximately B-centered (see Fig. 5) so that the $h + l$ odd reflections are systematically weak. The structure, however, was solved and refined without difficulty. The magnitude of the largest correlation coefficient that does

¹ Supplementary data for this paper are available from the IUCr electronic archives (Reference: BS0015). Services for accessing these data are described at the back of the journal.

Table 1
Experimental details.

	FLDNB	FLDNB2A	FLDNB2B	FLDNB2C
Crystal data				
Chemical formula	C ₂₅ H ₁₄ N ₂ O ₄	C ₂₅ H ₁₄ N ₂ O ₄	C ₂₅ H ₁₄ N ₂ O ₄	C ₂₅ H ₁₄ N ₂ O ₄
Chemical formula weight	406.38	406.38	406.38	406.38
Cell setting, space group	Monoclinic, <i>P</i> ₂ ₁ / <i>c</i>	Monoclinic, <i>P</i> ₂ ₁ / <i>c</i>	Monoclinic, <i>P</i> ₂ ₁ / <i>c</i>	Monoclinic, <i>P</i> ₂ ₁ / <i>c</i>
<i>a</i> , <i>b</i> , <i>c</i> (Å)	7.758 (1), 15.550 (2), 17.179 (2)	15.444 (3), 15.513 (4), 17.111 (4)	15.383 (2), 15.424 (3), 17.026 (3)	15.372 (2), 15.414 (3), 17.004 (3)
β (°)	110.72 (1)	110.04 (1)	109.31 (1)	109.24 (1)
<i>V</i> (Å ³)	1938.4 (4)	3851.3 (15)	3812.5 (11)	3804.0 (11)
<i>Z</i>	4	8	8	8
<i>D_x</i> (Mg m ⁻³)	1.393	1.402	1.416	1.419
Radiation type	Mo <i>K</i> α	Mo <i>K</i> α	Mo <i>K</i> α	Mo <i>K</i> α
No. of reflections for cell parameters	19 567	18 571	20 988	19 582
θ range (°)	2.8–27.8	1.0–25.0	1.0–25.0	1.0–25.0
μ (mm ⁻¹)	0.096	0.097	0.098	0.098
Temperature (K)	293 (1)	295 (1)	273 (1)	250 (1)
Crystal form, color	Prism, dark orange	Prism, dark orange	Prism, dark orange	Prism, dark orange
Crystal size (mm)	0.27 × 0.27 × 0.21	0.50 × 0.20 × 0.20	0.50 × 0.20 × 0.20	0.50 × 0.20 × 0.20
Data collection				
Diffractometer	Nonius KappaCCD	Nonius KappaCCD	Nonius KappaCCD	Nonius KappaCCD
Data collection method	φ and ω scans with 1.0° steps	φ and ω scans with 2.0° steps	φ and ω scans with 2.0° steps	φ and ω scans with 2.0° steps
No. of measured, independent and observed parameters	6214, 3403, 2584	12 155, 6757, 4236	12 796, 6689, 4893	12 862, 6674, 4932
Criterion for observed reflections	<i>I</i> > 2 σ (<i>I</i>)	<i>I</i> > 2 σ (<i>I</i>)	<i>I</i> > 2 σ (<i>I</i>)	<i>I</i> > 2 σ (<i>I</i>)
<i>R</i> _{int}	0.021	0.031	0.029	0.026
θ _{max} (°)	25.00	25.0	25.0	25.0
Range of <i>h</i> , <i>k</i> , <i>l</i>	−9 → <i>h</i> → 0 −18 → <i>k</i> → 18 −19 → <i>l</i> → 20	−18 → <i>h</i> → 18 −18 → <i>k</i> → 16 −20 → <i>l</i> → 20	−18 → <i>h</i> → 18 −18 → <i>k</i> → 18 −20 → <i>l</i> → 20	−18 → <i>h</i> → 18 −18 → <i>k</i> → 17 −20 → <i>l</i> → 20
Refinement				
Refinement on	<i>F</i> ²	<i>F</i> ²	<i>F</i> ²	<i>F</i> ²
<i>R</i> [<i>F</i> ² > 2 σ (<i>F</i> ²)], <i>wR</i> (<i>F</i> ²), <i>S</i>	0.066, 0.167, 1.06	0.076, 0.191, 1.06	0.052, 0.13, 1.06	0.051, 0.126, 1.06
No. of reflections and parameters used in refinement	3403, 280	6757, 559	6689, 559	6674, 559
H-atom treatment	Constrained	Constrained	Constrained	Constrained
Weighting scheme	$w = 1/[\sigma^2(F_o^2) + (0.062P)^2 + 1.2P]$, where $P = (F_o^2 + 2F_c^2)/3$	$w = 1/[\sigma^2(F_o^2) + (0.074P)^2 + 2.0P]$, where $P = (F_o^2 + 2F_c^2)/3$	$w = 1/[\sigma^2(F_o^2) + (0.053P)^2 + 1.24P]$, where $P = (F_o^2 + 2F_c^2)/3$	$w = 1/[\sigma^2(F_o^2) + (0.049P)^2 + 1.5P]$, where $P = (F_o^2 + 2F_c^2)/3$
(Δ/σ) _{max}	0.000	0.001	0.001	0.000
$\Delta\rho$ _{max} , $\Delta\rho$ _{min} (e Å ⁻³)	0.22, −0.23	0.32, −0.2	0.25, −0.2	0.23, −0.2

	PSEUFLDA	FLTIPS	PSEUTIPS
Crystal data			
Chemical formula	C ₂₅ H ₁₄ N ₂ O ₄	C ₂₈ H ₃₂ Si	C ₂₈ H ₃₂ Si
Chemical formula weight	406.38	396.63	396.63
Cell setting, space group	Monoclinic, <i>P</i> ₂ ₁ / <i>c</i>	Triclinic, <i>P</i> $\bar{1}$	Triclinic, <i>B</i> $\bar{1}$
<i>a</i> , <i>b</i> , <i>c</i> (Å)	7.722 (2), 15.513 (4), 17.111 (4)	8.012 (1), 16.171 (2), 18.280 (2)	8.012 (1), 16.171 (2), 18.280 (2)
α , β , γ (°)	90, 110.04 (1), 90	80.78 (1), 83.45 (1), 84.07 (1)	80.78 (1), 83.45 (1), 84.07 (1)
<i>V</i> (Å ³)	1925.6 (8)	2313.8 (5)	2313.8 (5)
<i>Z</i>	4	4	4
<i>D_x</i> (Mg m ⁻³)	1.402	1.139	1.139
Radiation type	Mo <i>K</i> α	Mo <i>K</i> α	Mo <i>K</i> α
No. of reflections for cell parameters	18 571	27 832	27 832
θ range (°)	1.0–25.0	2.6–27.8	2.6–27.8
μ (mm ⁻¹)	0.097	0.113	0.113
Temperature (K)	295 (1)	294 (1)	294 (1)
Crystal form, color	Prism, dark orange	Tablet, pale yellow	Tablet, pale yellow
Crystal size (mm)	0.50 × 0.20 × 0.20	0.58 × 0.53 × 0.37	0.58 × 0.53 × 0.37
Data collection			
Diffractometer	Nonius Kappa–CCD	Nonius Kappa–CCD	Nonius Kappa–CCD
Data collection method	φ and ω scans with 2.0° steps	φ and ω scans with 1.0° steps	φ and ω scans with 1.0° steps
No. of measured, independent and observed parameters	6094, 3377, 2505	8039, 8038, 7133	3988, 3988, 3640
Criterion for observed reflections	<i>I</i> > 2 σ (<i>I</i>)	<i>I</i> > 2 σ (<i>I</i>)	<i>I</i> > 2 σ (<i>I</i>)
<i>R</i> _{int}	0.021	0.035	0.031

Table 1 (continued)

	PSEUFLDA	FLTIPS	PSEUTIPS
θ_{\max} (°)	25.0	25.0	25.0
Range of h, k, l	−9 → h → 9 −18 → k → 16 −20 → l → 20	0 → h → 9 −18 → k → 19 −21 → l → 21	0 → h → 9 −18 → k → 19 −21 → l → 21
Refinement			
Refinement on	F^2	F^2	F^2
$R[F^2 > 2\sigma(F^2)], wR(F^2), S$	0.086, 0.185, 1.03	0.055, 0.144, 1.06	0.082, 0.206, 1.03
No. of reflections and parameters used in refinement	3377, 280	8038, 551	3988, 271
H-atom treatment	Constrained	Mixed	Constrained
Weighting scheme	$w = 1/[\sigma^2(F_o^2) + (0.042P)^2 + 3.3P]$, where $P = (F_o^2 + 2F_c^2)/3$	$w = 1/[\sigma^2(F_o^2) + (0.061P)^2 + 0.97P]$, where $P = (F_o^2 + 2F_c^2)/3$	$w = 1/[\sigma^2(F_o^2) + (0.089P)^2 + 3.9P]$, where $P = (F_o^2 + 2F_c^2)/3$
$(\Delta/\sigma)_{\max}$	0.001	0.000	0.000
$\Delta\rho_{\max}, \Delta\rho_{\min}$ (e Å ^{−3})	0.38, −0.4	0.3, −0.33	0.32, −0.54

not involve one of the disordered atoms of the isopropyl groups is 0.60. The isopropyl groups in one of the two molecules are disordered with occupancy factors 0.641/0.359 (3). These values are close enough to 2/3 and 1/3 to suggest an even larger unit cell, but we found no evidence of any additional scattering. The positions of the pairs of atoms C22B/C22X, C25B/C25X and C28B/C28X are sufficiently similar that their bond lengths to C20B, C23B and C26B had to be restrained [6 restraints; target length 1.53 (1) Å].

2.2. FLDNB and FLDNB2

Crystals were grown at 273 K from a hexane solution. Crystals are longest along a ; important faces belong to the forms {011} and {010}. Data were measured first on a Nonius CAD4 diffractometer at room temperature in July 1997. Connectivity was established (Xia, 1998), but the atomic ellipsoids were so eccentric and the data so weak [only 56% of the reflections had $I > 2\sigma(I)$] that the structure (hereafter, FLDNB) was put aside. Data were measured again, at 293 (1) K, shortly after the CCD diffractometer was installed (May 1998), but the results were only slightly more satisfactory. Two years passed. During that time software (routine PRECESSION in the program suite, COLLECT; Nonius, 1998) became available for transforming data from the unintegrated frames to projections of slices of the full diffraction pattern, *i.e.* to projections that resemble precession photographs. Careful inspection of projections nkl , hnl and hkn , $n = 0-3$, showed occasional ‘smudges’ at half-integral h . Three or four of these symmetrical regions of enhanced diffuse scattering were distinct enough to be considered as possible, but very diffuse, reflections. We decided to try to collect data at low temperature.

The vial of crystals had been stored in a laboratory drawer at room temperature. When we looked at them again (April 2000) they looked unchanged and all seemed to have the same habit. Five more crystals were mounted on the diffractometer. The first two were cooled immediately to 173 (2) K. They had the same unit cell found previously, except for a doubling of the a axis, but shattered before data collection could be

completed. The other three crystals were examined first at 295 (1) K, where the doubled axis was also found. Data for one of these crystals was measured at 295 (1), 273 (1) and 250 (1) K (structures identified hereafter as FLDNB2A, FLDNB2B and FLDNB2C), but the crystal shattered when cooled to 173 K.

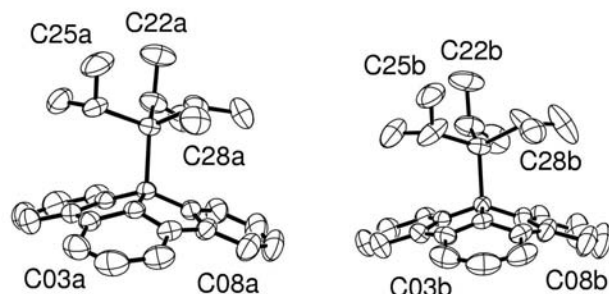
We had some difficulty solving the FLDNB2 ($Z' = 2$) structure, but no difficulty refining it. The magnitude of the largest correlation coefficient at 295 K is 0.74. At the lower temperatures the magnitude of the largest correlation coefficient is 0.62.

3. Molecular geometry

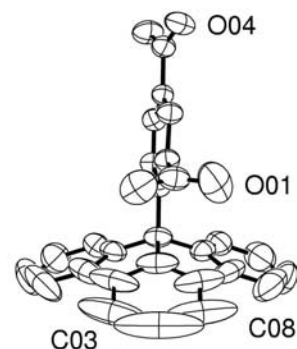
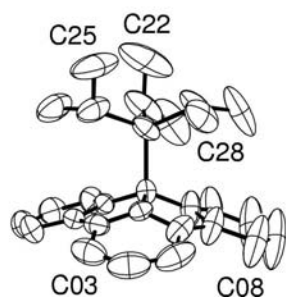
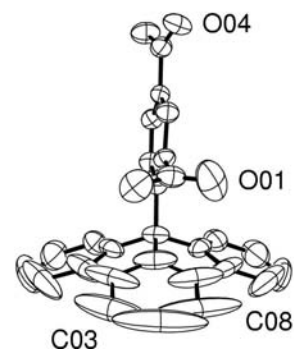
The intramolecular distances and angles for FLDNB and FLDNB2A are unreliable because of the large displacements of the atoms, as are the distances in the isopropyl groups of FLTIPS. The distances and angles for the C₁₉H₁₁Si fragment of FLTIPS, however, and for the whole molecule of FLDNB2C (250 K) are well determined. In each case the distances and angles are internally consistent over the two halves of the two independent molecules (*i.e.* 4 measurements for most values). For the fluoradene ring systems of these two structures the s.u.s are *ca.* 0.003 Å and 0.2° for the individual distances and angles, and less than 0.004 Å and 0.5° for the mean values. There are small (*ca.* 0.01 Å) differences between the values found in this study and the values determined for unsubstituted fluoradene (Dietrich *et al.*, 1975), but the values for unsubstituted fluoradene are almost certainly more accurate because the data for the latter were measured at 113 K to $\sin \theta/\lambda = 0.86$ Å and the atomic displacement ellipsoids are both small and physically reasonable. We do not believe we can see any variation in the geometry of the C₁₉H₁₁ ring system with a change in the C13 substituent.

The curvature of the fluoradene ring system is most easily assessed by considering the angle C12–C13–C14, which decreases as the curvature increases. This angle is 132.0 (1)° in the unsubstituted molecule, 129.3 (2) and 129.7 (2)° in the two independent molecules of FLTIPS, and 127.0 (2) and

FLTIPS



FLDNB

FLTIPS
(pseudocell
refinement)FLDNB2A
(pseudocell
refinement)**Figure 2**

Perspective drawing of molecules of FLTIPS as determined in the refinement of the true unit cell (upper drawings) and the B-centered pseudocell (lower drawing). The shapes of the ellipsoids of the non-H atoms correspond to 50% probability contours of atomic displacement. The H atoms have been omitted, as have the minor components of the disordered isopropyl groups. The atom numbers can be deduced from the atom labels shown and from Fig. 1.

128.1 (2)° in FLDNB2C. Another measure of the curvature is the angle between the least-squares planes of the rings composed of atoms C7–C12 and C14–C19. This angle is 34.5° in the unsubstituted molecule, 35.9 and 35.2° in FLTIPS, and 40.1 and 35.8° in FLDNB2C (all s.u.s 0.1°).

4. Crystal packing

The curvature of the fluoradene ring system hinders crystal packing; the number of ways molecules can fit together and still fill the space on the concave side of the fluoradene moiety is limited. If the substituent at C13 is just the right size to fill that cavity then columns can be formed, which is what happens in the FLTIPS structure (see Fig. 6). The columns are then arranged approximately hexagonally. The dinitrophenyl substituent of the FLDNB and FLDNB2 structures, however, cannot fill the space on the concave side of the fluoradene moiety in the same way. In the FLDNB and FLDNB2 structures pairs of inversion-related fluoradene ring systems enclose a region (see Fig. 7) which is filled by the dinitrobenzene substituents of two other inversion-related mole-

Figure 3

Perspective drawing of a molecule of FLDNB ($Z' = 1$; upper drawings) and of a molecule of FLDNB2A ($Z' = 2$; 295 K), as determined in the pseudocell refinement (lower drawing). The shapes of the ellipsoids of the non-H atoms correspond to 50% probability contours of atomic displacement. The H atoms have been omitted. The atom numbers can be deduced from the atom labels shown and from Fig. 1.

cules. The C13–C20 vectors of the two types of molecules are approximately perpendicular.

The difference in the melting points (413 K for FLTIPS; 513 K for FLDNB/FLDNB2) suggests that the crystal packing in the latter is more favorable, but the packing efficiencies of all structures as estimated by the VOID instruction of *PLATON* (Spek, 2000) are very low (0.658 for FLTIPS; 0.676 for FLDNB; 0.680 and 0.692 for FLDNB2A and FLDNB2C). The much greater polarity of the dinitrophenyl substituent compared with the triisopropylsilyl substituent must contribute substantially to the higher melting point(s) of the FLDNB and FLDNB2 crystals.

We found only three fluoradene structures in the April 2000 version of the Cambridge Structural Database (Allen & Kennard, 1993). One of these is a Li^+ salt of the anion formed by removing the substituent at C13 so that the ring system is planar (Bladauski *et al.*, 1979). The other two structures are the parent compound (Dietrich *et al.*, 1975) and the compound formed by replacing the H atom at C13 with an $\text{Re}(\text{CO})_5$ unit (Trifonova *et al.*, 1989). Two other structures, the trifluoromethanesulfonate salts of the *exo*- and *endo*- isomers of $[\text{Ru}(\eta^6\text{-fluoradene})(\eta^5\text{-C}_5\text{Me}_5)]$ have been published recently

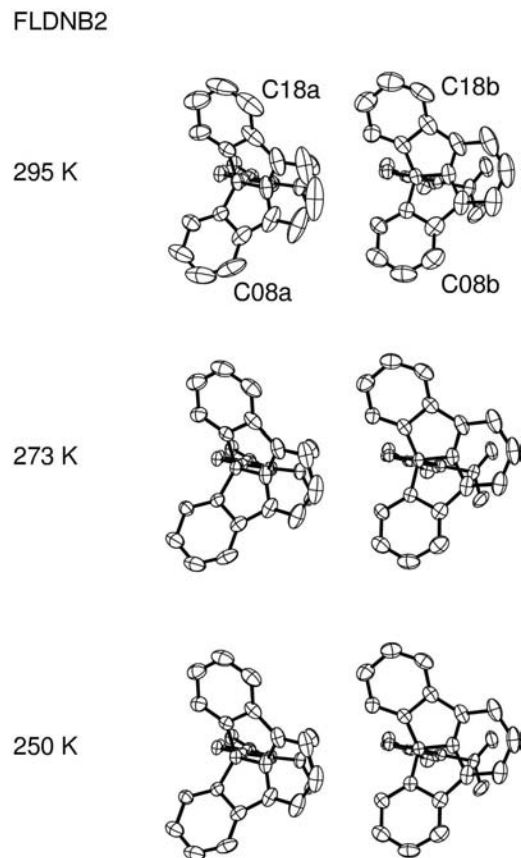


Figure 4
Perspective drawings of the molecule of FLDNB2 ($Z' = 2$) at three temperatures. The shapes of the ellipsoids of the non-H atoms correspond to 50% probability contours of atomic displacement. The H atoms have been omitted. The atom numbers can be deduced from the atom labels shown and from Fig. 1.

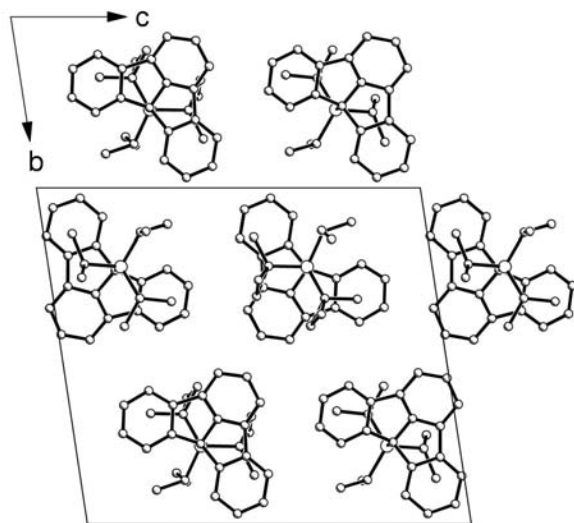


Figure 5
Projection parallel to **a** of a slice of the FLTIPS structure. Note that the **b** and **c** axes point out of the plane of the drawing. Molecules separated by $\Delta z \approx 1/2$ are also separated by $\Delta x \approx 1/2$.

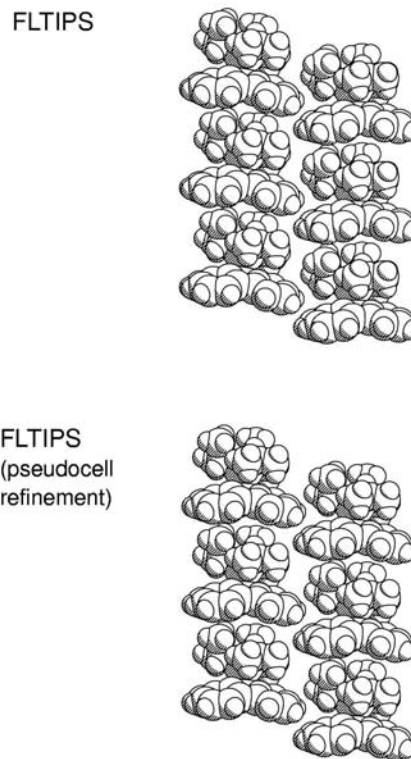


Figure 6
Projection showing two stacks of FLTIPS molecules in the actual structure (upper drawing) and in the pseudostructure (lower drawing). The **a** axis points vertically upwards and the **c** axis points to the right. In the upper drawing the column on the left is composed exclusively of molecule *A* and the column on the right is composed exclusively of molecule *B*. The van der Waals radii of the atoms have been reduced (Si, 1.67 Å; C, 1.27 Å; H, 0.82 Å) to clarify the drawing.

(Xia *et al.*, 2000). Structures of two derivatives of the *exo* isomer, *i.e.* the trifluoromethanesulfonate salts with methyl and isopropyl substituents at C13, have been determined (Xia, 1998) but not yet published.

Like FLTIPS, the structures of the salts of the *exo* and *endo* isomers of the $\text{Ru}(\eta^5\text{-C}_5\text{Me}_5)$ complex of fluoradene (coordination is to the two different sides of the C1–C6 ring) contain columns in which the molecules are related by translation. The orientation of the fluoradene ring system with respect to the column axis, however, is slightly different from that found here. In FLTIPS the C13–Si vector is nearly parallel to **a** [angles C13–Si ··· C13 are 167.6 (1) and 176.3 (1)° for molecules *A* and *B*]. In the pair of *exo/endo* isomers it is the vector from the midpoint of the C1–C6 ring to the Ru atom and the Ru–C₅Me₅ vector that are nearly aligned with a cell edge.

In unsubstituted fluoradene there is little overlap of the ring systems when the structure is projected on the least-squares molecular plane. In the structures of the $\text{Re}(\text{CO})_5$ derivative and of the trifluoromethanesulfonate salts of the methyl and isopropyl derivatives (*i.e.* the other molecules that do not stack into columns) the concave surfaces of two fluoradenes are in direct contact.

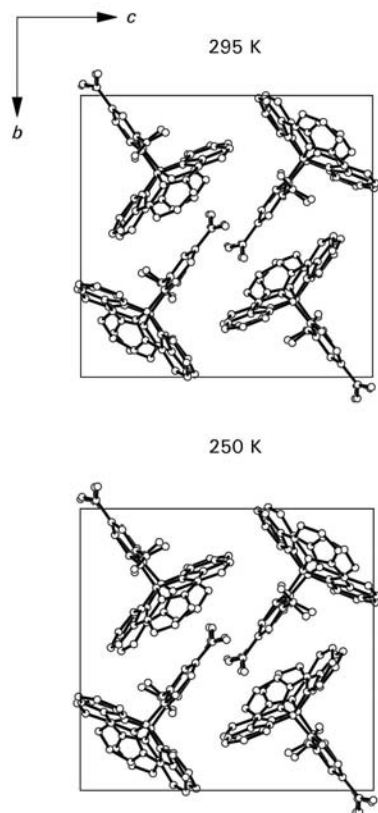


Figure 7

Projection parallel to **a** of the FLDNB2 structure ($Z' = 2$) at 295 and 250 K. Note that the **c** axis points into the plane of the drawing; the apparent repeat in the horizontal direction is $c \sin \beta$. Molecules separated by $\Delta x \simeq 1/2$ are crystallographically independent. Note also that the dinitrophenyl fragments of the two molecules are very nearly superimposed, but that the orientations of the fluoradene ring systems differ noticeably.

5. How pseudosymmetric are the structures?

Three approaches to assessing the degree of pseudosymmetry in the FLTIPS and FLDNB2 structures were tried. First, the atomic coordinates were analyzed. Second, least-squares refinements were carried out in the smaller pseudocells. Third, separate Wilson plots for the odd and even reflections were made for each structure. The three methods are all informative, but in different ways.

5.1. Analyses of coordinates

Least-squares fits of coordinates of related molecules and fragments were made using the OFIT command in routine XP of Sheldrick's (1990) program package *SHELXTL/PC*. For each structure the fit was made first for all atoms, then for the atoms of the fluoradene ring system plus the atom attached to C13 (C1–C19 plus Si or C20), and finally for all atoms of the substituent on the fluoradene ring system (all atoms less C1–C12 and C14–C19). For FLTIPS the r.m.s. deviations are 0.06, 0.04 and 0.06 Å, respectively, for the molecule and the two

fragments; these very small deviations show that the two molecules can be superimposed almost exactly. For FLDNB2A, FLDNB2B and FLDNB2C the deviations are 0.26, 0.34 and 0.35 Å for all atoms, 0.06, 0.08 and 0.08 Å for the fluoradene ring system, and 0.08, 0.11 and 0.12 Å for the dinitrophenyl ring. The larger deviations for the FLDNB2X molecules result from the slightly different torsion angles around the bonds (C13–C20) that connect the two ring systems [1.2 (4) and 16.2 (3)° for the two molecules averaged over the three temperatures]. The larger deviations in the dinitrophenyl ring reflect the slightly different torsion angles around the bond to the *ortho*-nitro group (C21–N1) in the two molecules [106.4 (10) and 92.5 (3)° for the two molecules averaged over the three temperatures]. The corresponding angles for the *para*-nitro group (C23–N2) are more similar [15.9 (1) and 16.3 (2)°].

Fits of the molecules related by pseudosymmetry were also made using the instruction FIT in the program *PLATON* (Spek, 2000). In FLTIPS the molecular centers of gravity are related by the vector $\frac{1}{2} + 0.037, -0.003, \frac{1}{2} - 0.002$; the displacements from the ideal values are 0.29, -0.04 and -0.04 Å, and the relative rotation of the molecules is 9.3°. In FLDNB2A the vector that relates the centers of gravity is $\frac{1}{2} - 0.007, 0.009, -0.011$, the displacements are $-0.10, 0.13$ and -0.18 Å, and the rotation is 9.4°. The two molecules in FLTIPS are more similar than the two molecules in FLDNB2A, but the pseudotranslational symmetry is more perfect in FLDNB2A than in FLTIPS.

5.2. Pseudocell refinements

Pseudocell refinements were performed for FLTIPS and FLDNB2A. For the former the $h + l$ odd reflections were discarded, the space group was changed from $P\bar{1}$ to $B\bar{1}$, and the second molecule was discarded. For FLDNB2A the h odd reflections were discarded and the h indices of the corresponding even reflections were halved. The unit-cell dimension a was halved, the x coordinates of the first molecule were doubled and the entire second molecule was discarded. The refinements then proceeded normally (see Figs. 2 and 3 and Table 1). The agreement factors are surprisingly, and perhaps rather alarmingly, satisfactory. The ellipsoid plots show where the differences between the two independent molecules are localized. In FLTIPS the molecules are most different in the region of C7–C11; one molecule is slightly tipped relative to the other. The atomic ellipsoids are also all a little larger in the pseudocell refinement. In FLDNB2A the fluoradene ring system is affected by a rotation around the bond that connects the two types of ring systems (C13–C20). Since the atomic ellipsoids of the dinitrophenyl moiety are normal, the rotation must be an internal rotation rather than a motion of the molecule as a whole.

The ellipsoid plots for FLDNB and for FLDNB2A as refined in the pseudocell (see Fig. 3) are strikingly similar. The two sets of data, however, are clearly different. Careful scrutiny (see above) of the precession-like projections of the FLDNB reciprocal lattice showed only a few areas of diffuse

scattering at half-integral h ; there were no defined peaks at those locations. There is no doubt at all that the projections for FLDNB and FLDNB2A differ.

The pseudocell refinements suggest that the degree of pseudosymmetry in the FLTIPS and FLDNB structures is comparable. The agreement factors R_1 and wR_2 are similar (0.082 and 0.206 for FLTIPS; 0.086 and 0.185 for FLDNB2A) and the eccentricities of the ellipsoids are similar. The ellipsoids of FLTIPS do, however, look slightly 'better', which might suggest that FLTIPS is the more symmetric structure even though its wR_2 value is a little higher.

5.3. Wilson plots

Separate Wilson plots (bin width 0.02 \AA^{-2}) were made for the reflections that are odd and even in the directions of the cell doubling (see Figs. 8 and 9). These plots show the effects of the pseudosymmetry clearly; the parameters for the associated least-squares lines (first and last point excluded) allow quantitative comparisons. A striking feature is the difference in the slopes of these lines. The geometric part of the structure factors for the odd reflections increases with scattering angle because the differences between the two molecules become more important with increasing resolution. The fall-off in intensity resulting from the thermal motion (and disorder in the case of FLTIPS) keeps the slope of the lines for the odd reflections from being positive, but the slope is substantially less negative for the odd than for the even reflections.²

Since the slopes for the two lines are different, it is less useful than one might hope to make a simple comparison of the average intensity of the odd and even reflections. It is better to compare the average intensity at some fixed scattering angle. For FLTIPS the difference between even and odd reflections at $\theta = 0^\circ$ is 0.74 (8) on the \log_{10} scale; the intensity ratio is therefore ~ 5 (1). For FLDNB2A (295 K) the difference is 1.40 (7), so that the intensity ratio is 25 (4). The corresponding values for FLDNB2C (250 K) are 0.98 (9) and 10 (2).³ The Wilson plots show that FLDNB2 becomes less pseudosymmetric as the temperature is lowered, but that even at 250 K FLDNB2 is still somewhat more pseudosymmetric than FLTIPS.

Taken together the three measures of pseudosymmetry give a good description of the structural distortions associated with the cell doubling. In FLTIPS the two molecules have very nearly the same conformation; the differences are localized in the translation of the whole molecule along **a** and the rotation of the molecule around **b** (see Figs. 5 and 6). In FLDNB2 the two molecules have somewhat different conformations, but the average molecules are very nearly superimposed by the

² Experience with plots for these and other structures suggests that the greater intensity differences between strong and weak reflections are correlated with a larger difference in the slopes of the two least-squares lines. In principle, the slope for the weak reflections could even be positive, but we have never seen that happen.

³ Comparisons might also be made at $\sin^2\theta/\lambda^2 = 0.10 \text{ \AA}^{-2}$ or $\theta = 13^\circ$ for Mo $K\alpha$ radiation, because that is the region that might be examined with photographic films. For FLTIPS the intensity ratio at 0.10 \AA^{-2} is 4 (see caption to Fig. 8). For FLDNB2A and FLDNB2C the intensity ratios at 0.10 \AA^{-2} are 11 and 5 (see caption to Fig. 9).

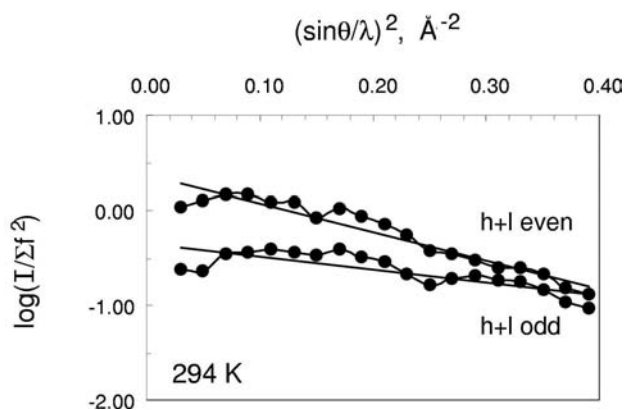


Figure 8

Wilson plots for the $h + l$ even and $h + l$ odd reflections of FLTIPS. The slopes of the $h + l$ even and $h + l$ odd lines are -3.0 (2) and -1.3 (2) \AA^2 ; the corresponding intercepts are $+0.38$ (5) and -0.35 (6).

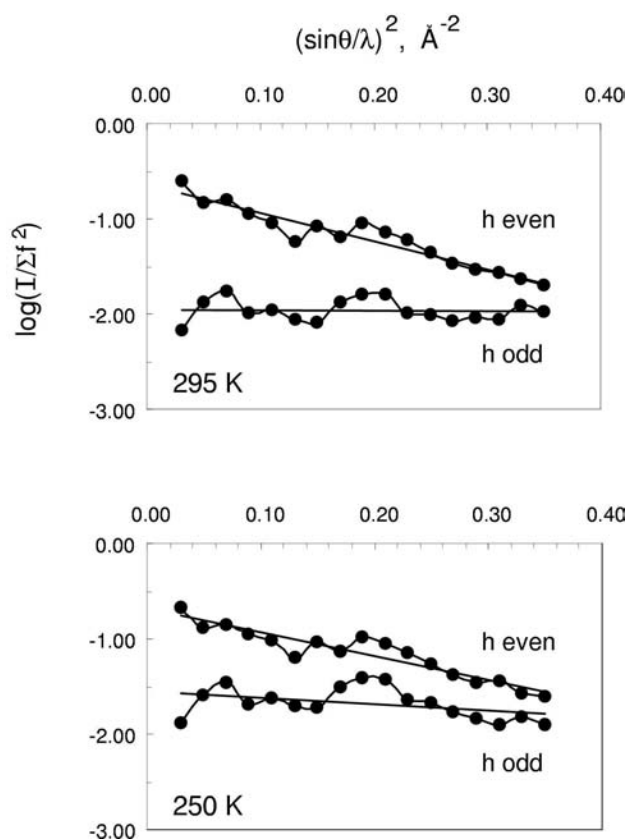


Figure 9

Wilson plots for the h even and h odd reflections of FLDNB2A and FLDNB2C. The slopes of the h even and h odd lines are -3.0 (3) and -0.0 (3) \AA^2 at 295 K, and are -2.4 (3) and -0.5 (4) \AA^2 at 250 K. The intercepts are -0.64 (5) and -1.97 (7) at 295 K, and are -0.71 (5) and -1.59 (9) at 250 K.

pseudotranslation. At low resolution the differences between the molecular conformations are less important than the distortions from translational symmetry and so the Wilson plots for the FLTIPS structure (Fig. 8) look less pseudosymmetric than those for the FLDNB2 structure (Fig. 9). The differences between the two classes of reflections are substantially smaller for the FLTIPS crystal than for the FLDNB2A crystal.

Note that very small distortions from translations, glides and screw rotations have very large consequences for whole classes of reflection intensities. Even if the atomic displacements associated with a structural distortion are small enough (*ca.* 0.1–0.2 Å) to be absorbed into the atomic displacement parameters, it is often easy to measure the effects of those displacements on the intensities that would be zero in a cell with a smaller asymmetric unit. If a full set of intensity data is available and if the molecules are related approximately by an operation that includes a translation, then distinguishing between a true $Z' > 1$ structure and a structure refined in too large a asymmetric unit is usually straightforward. Making this kind of distinction is much easier than distinguishing between real and approximate inversion centers (see, *e.g.*, Marsh, 1999).

6. Notes on the cell settings

The reduced cell for the FLDNB structure ($Z' = 1$) corresponds to space group $P2_1/n$ [$c = 16.156(2)$ Å; $\beta = 95.97(1)^\circ$] rather than $P2_1/c$; the $P2_1/c$ setting was chosen because of its simpler relationship ($\frac{1}{2}00, 010, 001$) to the reduced $P2_1/c$ cell of the FLDNB2 ($Z' = 2$) superstructure. Note that doubling the **a** axis of the $P2_1/n$ cell of FLDNB does not lead to the same superstructure as doubling the **a** axis of the $P2_1/c$ cell; the hkl, l even, reflections of the two possible superstructures would be superimposable but the hkl, l odd reflections would not. There is, of course, a $P2_1/n$ cell [$c = 18.713(4)$ Å; $\beta = 120.79(1)^\circ$] for the $Z' = 2$ superstructure that is derived from the $P2_1/c, Z' = 2$ cell by the transformation $(\bar{1}00, 0\bar{1}0, 101)$, but that cell is not the same as the $P2_1/n$ cell derived by doubling the **a** axis of the $P2_1/n, Z' = 1$ cell [$c = 16.156(2)$ Å; $\beta = 95.97(1)^\circ$].

Cell/supercell relationships can be very confusing. If the $P2_1/n$ structure of FLDNB had already been in the literature it would have been easy to have missed its close relationship to the $P2_1/c$ structure of FLDNB2. It seems likely that the CSD (Cambridge Structural Database) already contains pairs of structures whose similarities are obscured by the differences between their reduced cells.

Cell/supercell relationships become even more confusing if the crystal system is triclinic. If the FLTIPS cell really were B-centered the reduced cell would have obtuse, rather than acute, angles. The cell parameters would be $a = 8.012(1)$, $b = 9.552(2)$, $c = 16.171(2)$ Å, and $\alpha = 96.31(1)$, $\beta = 95.93(1)$ and $\gamma = 108.07(1)^\circ$.

7. Why doesn't $Z' = 1$? Should $Z' = 1$?

Only ~7% of the structures in the CSD have more than one molecule in the asymmetric unit (Brock & Dunitz, 1994). The true frequency of $Z' > 1$ structures is undoubtedly somewhat higher because superstructure reflections may be overlooked and refinement difficulties may hinder publication. Still, structures with $Z' > 1$ are the exception rather than the rule.

The preference for a smaller asymmetric unit may be related to the shape of atom–atom potential functions, which are steeply repulsive at small distances, significantly repulsive in the region of van der Waals contacts and weakly attractive at long distances. Consider, for example, the H···H potential Π (optimized partial charges) of Williams & Starr (1977), which is calibrated for C–H distances lengthened to 1.040 Å (1.027 Å for aromatic C atoms). An H···H contact at the conventional van der Waals sum of 2.40 Å corresponds to an energy of 0.77 kJ mol⁻¹. If the one contact of 2.40 Å is split into two contacts of 2.30 and 2.50 Å, then the energy rises to 0.85 kJ mol⁻¹. To bring the energy of that one set of contacts back to the original value the structure could expand slightly, but the expansion would also decrease the long-range attractions (the structure would be slightly less dense) and would therefore raise the overall energy. Doubling the number of interactions by doubling Z' is not expected to be favorable.

Many of the structures in the CSD that have $Z' > 1$ were studied at low temperature. Phase transitions that occur during cooling and that are associated with an integral multiplication of the cell volume are no surprise; classic examples are biphenyl (Baudour, 1991; Lenstra *et al.*, 1994, and references therein) and ferrocene (Seller & Dunitz, 1979; Dunitz, 1993). These transitions are often the result of a 'short' atom–atom contact that is acceptable when the temperature is higher and the vibrational amplitudes larger, but that becomes increasingly unfavorable as the vibration amplitudes decrease (see Busing, 1983). Perhaps, maybe even probably, there exists for each $Z' > 1$ structure another crystal form with $Z' = 1$ that has an even lower energy (see Dunitz *et al.*, 2000, and references therein), but the chances of transformation to an entirely new phase with retention of crystallinity (a condition usually required if the structure is to end up in a crystallographic database) are extremely small. The transformations that are actually observed nearly always involve small structural shifts that result in larger, pseudosymmetric unit cells.

The unusual feature of the two $Z' = 2$ structures described here is that they were studied at temperatures above, rather than below, the temperatures of crystal growth. There was no chance that a phase transition associated with crystal cooling took place.

8. Are the FLDNB and FLDNB2 structures polymorphs?

To what extent should the two FLDNB structures be considered to be the same and what is the order of the phase transition that relates them?

The transition of FLDNB to FLDNB2 is clearly an order–disorder transition, but it is more difficult to say whether it

should be viewed as a first- or second-order transition. The volume change near 295 K is large enough [-0.66 (3)%] to indicate a first-order transition, but the additional ΔV of -1.01 (2)% between 295 and 273 K shows that the transition continues over a temperature range, which behavior is typical of a second-order transition. The phase behavior between room temperature and 273 K is not simple. There does not seem to be any major change in the structure between 273 and 250 K, but some change must occur if the temperature is lowered further because all crystals cooled to 110 K shattered within hours.

The few very weak and very diffuse ‘reflections’ we could see for half-integral h in the precession projections of FLDNB ($Z' = 1$) suggest medium-to-long-range correlations of the type associated with the phase transition. The transition was perhaps in the first stages of nucleation. The relatively poorer refinement of the FLDNB2 structure at 295 K relative to the structures at 273 and 250 K suggests that at room temperature the crystal still contained large regions that were imperfectly ordered. The precession-like projections of slices of the reciprocal lattices (see §2.2) show that between 295 and 273 K the background scattering is much reduced and that the Bragg peaks become stronger and better defined.

If the two FLDNB phases were related by a simple order-disorder transition then it might be expected that the symmetry of the ordered phase would be lower than the symmetry of the disordered phase. Careful examination of the $h0l$ and $0k0$ reflections for FLDNB2C (at 250 K), indicates, however, that the structure is still best described in the space group $P2_1/c$.

It is tempting to think of the FLDNB structure ‘settling into’ the better ordered and more compact FLDNB2 structure during the 2 years the vial of crystals sat in a laboratory drawer. It is likely, however, that the reality is more complicated. The $P2_1/c$ cell constants for FLDNB measured with the CAD4 diffractometer in July 1997 were 7.701 (2), 15.481 (3), 17.070 (3) Å and 109.67 (2)°, which is to say that the dimensions for the doubled FLDNB2 cell lie *between* the dimensions measured for the two supposed FLDNB crystals. That observation suggests that the crystal studied in 1997 really had the FLDNB2 structure rather than the FLDNB structure, but that we missed the cell doubling. Perhaps a recrystallization was carried out but not recorded. Perhaps some of the ‘single’ crystals examined were actually hybrids of the two phases. Perhaps there was some other systematic error. Perhaps we would have found a FLDNB crystal in April 2000 if we had mounted yet more crystals on the diffractometer. These questions only serve to highlight the difficulties and frustra-

tions of studying phase relationships in molecular solids (see Sarma & Dunitz, 1990, for a similar example). What is certain is that two forms of the solid exist and that they are so closely related that distinguishing between them is difficult.

We thank the National Science Foundation (EPS-9452895 and MRSEC DMR-9809686) for financial support. AX thanks the University of Kentucky for a Graduate Fellowship and BOP thanks the same institution for a Postdoctoral Fellowship. We are grateful to Dr Y. Le Page, Dr R. E. Marsh, Professor C. E. Nordman and Professor A. L. Spek for very helpful correspondence.

References

- Allen, F. H. & Kennard, O. (1993). *Chem. Des. Autom. News*, **8**, 1, 31–37.
- Altomare, A., Cascarano, G., Giacovazzo, C., Guagliardi, A., Burla, M. C., Polidori, G. & Camalli, M. (1994). *J. Appl. Cryst.* **27**, 435–436.
- Baudour, J. L. (1991). *Acta Cryst.* **B47**, 935–949.
- Bladauski, D., Broser, W., Hecht, H.-J., Rewicki, D. & Dietrich, H. (1979). *Chem. Ber.* **112**, 1380–1391.
- Brock, C. P. & Dunitz, J. D. (1994). *Chem. Mater.* **6**, 1118–1127.
- Busing, W. R. (1983). *Acta Cryst.* **A39**, 340–347.
- Dietrich, H., Bladauski, D., Grosse, M., Roth, K. & Rewicki, D. (1975). *Chem. Ber.* **108**, 1807–1822.
- Dunitz, J. D. (1993). *Organic Chemistry: Its Language and Its State of the Art*, edited by M. V. Kisakuerek, pp. 9–23. Basel: Verlag Helvetica Chim Acta.
- Dunitz, J. D., Filippini, G. & Gavezzotti, A. (2000). *Helv. Chim. Acta*, **83**, 2317–2335.
- Lenstra, A. T. H., Alsenoy, C. V., Verhulst, K. & Geise, H. J. (1994). *Acta Cryst.* **B50**, 96–106.
- Marsh, R. E. (1999). *Acta Cryst.* **B55**, 931–936.
- Nonius (1998). *Collect Data Collection Software*. Nonius BV, Delft, The Netherlands.
- Otwinowski, Z. & Minor, W. (1997). *Methods Enzymol.* **276**, 307–326.
- Sarma, J. A. R. P. & Dunitz, J. D. (1990). *Acta Cryst.* **B46**, 784–794.
- Seller, P. & Dunitz, J. D. (1979). *Acta Cryst.* **B35**, 2020–2032.
- Sheldrick, G. M. (1990). *SHELXTL/PC*. Siemens Analytical Instruments, Inc., Madison, Wisconsin, USA.
- Sheldrick, G. M. (1997a). *SHELXS97*. University of Göttingen, Germany.
- Sheldrick, G. M. (1997b). *SHELXL97*. University of Göttingen, Germany.
- Spek, A. L. (2000). *PLATON*. Utrecht University, The Netherlands.
- Trifonova, O. I., Ustynyuk, Y. A., Ustynyuk, N. A., Oprunenko, Y. F., Batsanov, A. S. & Struchkov, Y. T. (1989). *Metalloorg. Khim.* **2**, 581–585.
- Williams, D. E. & Starr, T. L. (1977). *Comput. Chem.* **1**, 173–177.
- Xia, A. (1998). Ph.D. Thesis. University of Kentucky.
- Xia, A., Selegue, J. P., Carrillo, A. & Brock, C. P. (2000). *J. Am. Chem. Soc.* **122**, 3973–3974.

Coupling of the lactone-ring conformation with crystal symmetry in 6-hydroxy-4,4,5,7,8-pentamethyl-3,4-dihydrocoumarin. Erratum

Armand Budzianowski Andrzej Katrusiak,

Faculty of Chemistry, Adam Mickiewicz University, 60-780 Poznań, Grunwaldzka 6, 60-780 Poznan, Poland

In the paper by Budzianowski & Katrusiak (2002) *Acta Cryst.* (2002), B58, 125–133 Figs. 5 and 8 on pages 131 and 132 were transposed while adjusting colour details indicated by the authors in the proof. Revised PDF versions of these pages are available in the online version of this erratum, which is available through **Crystallography Journals Online**.

Two fluoradene derivatives: pseudosymmetry, eccentric ellipsoids and a phase transition. Erratum

Aibing Xia, John P. Selegue, Alberto Carrillo, Brian O. Patrick, Sean Parkin and Carolyn Pratt Brock*

Department of Chemistry, University of Kentucky, Lexington, KY 40506-0055, USA

Numerous printing errors in the paper by Xia *et al.* [*Acta Cryst.* (2001), B57, 507–516] are corrected.

In the paper by Xia *et al.* (2001) a number of special characters (', λ , Å, σ , Δ , ö) were omitted in the printed and PDF versions of the article; the HTML version, however, was correct. The corrected version of the paper is now available from **Crystallography Journals Online**.

References

Xia, A., Selegue, J. P., Carrillo, A., Patrick, B. O., Parkin, S. & Brock, C. P. (2001). *Acta Cryst.* B57, 507–516.

Group-Theoretical Analysis of Octahedral Tilting in Perovskites. Erratum

Christopher J. Howard^{a*} and Harold T. Stokes^b

^aAustralian Nuclear Science and Technology Organisation, Private Mail Bag 1, Menai NSW 2234, Australia, and ^bDepartment of Physics and Astronomy, Brigham Young University, Provo, Utah 84602-4675, USA

An error has been noted within Fig. 1 of the paper by Howard & Stokes (1998). There is a group–subgroup relationship between $I4/mcm$ ($a^0a^0c^-$) and $C2/c$ ($a^-b^-b^-$), and this should be indicated on the figure by a continuous line joining the corresponding boxes. The corrected version of the figure is shown here.

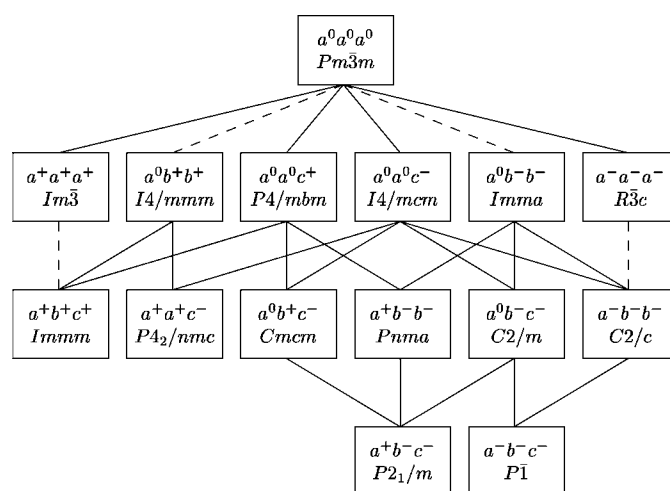


Figure 1

A schematic diagram indicating the group–subgroup relationships among the 15 space groups tabulated by Howard & Stokes (1998). A dashed line joining a group with its subgroup indicates that the corresponding phase transition is required by Landau theory to be first order.

References

Howard, C. J. & Stokes, H. T. (1998). *Acta Cryst.* B54, 782–789.